# Magnetic Resonance Studies of Polypeptides Adsorbed on Silica and Hydroxyapatite Surfaces

**Veronica L. Fernandez,† Jeffrey A. Reimer,* and Morton M. Denn**

*Contribution from the Center for Advanced Materials, Lawrence Berkeley Laboratory, and Department of Chemical Engineering, University of California at Berkeley, Berkeley, California 94720-9989.* *Received May 15, 1992*

**Abstract:** Solid-state $^{13}C$ and $^{2}H$ nuclear magnetic resonance were used to reveal differences in conformation and local mobility between polypeptides in the bulk-solid and surface-adsorbed states. Carbon-13 chemical shifts show that the $\alpha$-helical structures of longer chain solid poly-L-lysine and poly-L-glutamic acid are largely replaced by a more extended conformation upon adsorption. These shifts also identify specific side-chain functional group interactions with surface sites. Restriction of side-chain amino group rotation, revealed in $^{2}H$ NMR experiments, demonstrates the strength of these adsorbate–surface interactions. Measurements of $^{13}C$ rotating-frame spin-lock relaxation and cross-polarization dynamics indicate that, in general, both side-chain and backbone motions of adsorbed poly-L-lysine and poly-L-glutamic acid are diminished relative to the bulk-solid state. Taken together, these results suggest that the polypeptides adsorb in a flat, relatively extended conformation through strong electrostatic interactions of side-chain functional groups with the surface. This work demonstrates the effective use of conventional solid-state NMR analysis for studying conformational and motional behaviors of surface-adsorbed polymers.

## Introduction

Polymer and protein interactions with surfaces are important in many applications, including chromatography, biomedical devices, colloids, adhesion, composite materials, and polymer processing. Although protein and polymer adsorption behavior on solid surfaces has received considerable attention, research efforts in synthetic polypeptide adsorption are scarce. This is unfortunate since it is likely that the fundamental mechanisms involved in polypeptide/solid surface interactions are also of considerable influence in protein and polymer adsorption.

Of particular interest in studies of macromolecule adsorption are (1) the macromolecular conformation induced by adsorption on the surface, and (2) local dynamics or motional freedom of the adsorbed molecule. Solid-state nuclear magnetic resonance (NMR) spectroscopy is ideally suited for investigation of these questions because of its sensitivity to conformation (through the chemical shift) and to local dynamics (through characteristic relaxation times).

Many investigators have successfully employed solid-state NMR to describe bulk polymer structure and dynamics.[1-5] NMR is not, however, applied widely to surface studies because of its intrinsic low sensitivity. Most applications of NMR to surfaces have been studies of small gaseous molecules maximally loaded on high surface area catalysts.[6] While the potential for NMR studies of adsorbed polymers has been recognized since the early 1970's,[7] extremely low signal intensities and broad lines typical of the solid state have hindered research efforts, and few investigations have met with much promise. Several solid-state NMR studies of long-chain organics terminally grafted on surfaces[8,9] have been fruitful because the order-of-magnitude higher loadings and relatively short molecules (compared with polymers) allow for sufficient signal. For investigations of adsorbed polymers, however, high resolution liquid-state methods have thus far proven more informative than solid-state techniques. This is illustrated in recent work[10-12] in which liquid-state carbon and deuterium NMR are used to assess relative mobilities in the two blocks of a terminally-attached, solvent-swollen block copolymer. Only in the past few years have solid-state spectra of adsorbed polymers been achieved[13,14] with adequate resolution and signal-to-noise to warrant further studies.

The work presented here demonstrates the use of solid-state NMR techniques to compare both conformation and local dynamics of surface-adsorbed polymers with those of bulk solid polymers. In this study, two homopolypeptides, poly-L-glutamic acid (PG) and poly-L-lysine (PL), were adsorbed from aqueous solution onto precipitated silica and/or hydroxyapatite ($Ca_{10}(PO_4)_6(OH)_2$) surfaces. PL and PG are easily soluble in water and contain amino or carboxyl side-chain functional groups, respectively, that can be charged or neutral depending on pH. Lysine and glutamic acid residues occur with high frequency on the outer surfaces of many proteins, so their behavior at a solid surface is of particular interest as a model for protein adsorption. These polypeptides are also known to take on extended $\beta$-sheet, random coil, or $\alpha$-helix secondary conformations depending on such factors as chain length, solution pH, and solvent chemistry. Silica and hydroxyapatite (HA) are available as relatively high surface area powders for use in chromatography columns. Hydroxyapatite also shows promise as a highly biocompatible material with unique bioactive properties. The active surface sites of silica are predominantly SiOH and $SiO^-$ groups.[15] Those of HA are probably charged calcium or phosphate groups.[16-18]

While there is general agreement that PL and PG adsorb on silica and/or HA by electrostatic mechanisms, it is uncertain how the polymer conformation is affected by the adsorption. Conformational changes have been postulated[19-23] based on adsorption

* Corresponding Author.
† Bioengineering Program, University of California at San Francisco and Berkeley.

(1) Spiess, H. W. *Annu. Rev. Mater. Sci.* **1991**, *21*, 131.
(2) *NMR and Macromolecules. Sequence, Dynamics, and Domain Structure*; Randall, J. J. C., Ed.; ACS Symposium Series 247; American Chemical Society: Washington, DC, 1984.
(3) Slichter, W. P. In *NMR Studies of Solid Polymers*; Diehl, P., Fluck, E., Kosfeld, R., Eds.; Springer Verlag: New York, 1971; p 209.
(4) McBrierty, V. J. *Polymer* **1974**, *15*, 503.
(5) Havens, J. R.; Koenig, J. L. *Appl. Spectrosc.* **1983**, *37*, 226.
(6) Duncan, T. M.; Dybowski, C. *Surf. Sci. Rep.* **1981**, *1*, 157.
(7) Miyamoto, T.; Cantow, H. J. *Makromol. Chem.* **1972**, *162*, 43.
(8) Facchini, L.; Legrand, A. P. *Macromolecules* **1984**, *17*, 2405.
(9) Sindorf, D. W.; Maciel, G. E. *J. Am. Chem. Soc.* **1983**, *105*, 1848.
(10) Blum, F. D.; Sinha, B.; Schwab, F. C. *Polym. Mater. Sci. Eng.* **1988**, *59*, 302.
(11) Blum, F. D.; Sinha, B. R.; Schwab, F. C. *Macromolecules* **1990**, *23*, 3592.
(12) Blum, F. D.; Sinha, B. R.; Schwab, F. C. *Polymer Prepr., Am. Chem. Soc. Div. Polym. Chem.* **1991**, *32*, 271.
(13) Blum, F. D.; Funchess, R. B. *Polymer Prepr., Am. Chem. Soc. Div. Polym. Chem.* **1988**, *29*, 54.
(14) Blum, F. D.; Funchess, R. B.; Meesiri, W. In *Dynamics of Surface Bound Species*; Ishida, H., Ed.; Elsevier Science Publishing: New York, 1988; p 205.
(15) Iler, R. K. *Chemistry of Silica*; Wiley: New York, 1979.
(16) Bernardi, G.; Kawasaki, T. *Biochim. Biophys. Acta* **1968**, *160*, 301.
(17) Bernardi, G.; Giro, M.-G.; Gaillard, C. *Biochim. Biophys. Acta* **1972**, *278*, 409.
(18) Kresak, M.; Moreno, E. C.; Zahradnik, R. T.; Hay, D. I. *J. Colloid Interface Sci.* **1977**, *59*, 283.

0002-7863/92/1514-9634$03.00/0 

isotherms, adsorbed layer thicknesses, and electrophoretic mobility. Only one previous study[24] has observed the conformation of adsorbed polypeptide directly, using IR spectroscopy. This method, however, required that the sample be ground with a solvent and cast into a film before analysis.

This paper presents the results of solid-state NMR experiments which reveal conformational and motional information about poly-L-lysine and poly-L-glutamic acid adsorbed on silica and/or hydroxyapatite from aqueous solution. Carbon-13 chemical shifts provide a means of directly observing conformational differences between bulk-solid and surface-adsorbed PL and PG, and also allow identification of specific functional group interactions with the surface. Because quadrupolar line shapes reflect fast local motions, low-temperature deuterium experiments clearly reveal the reduced rotational rate of surface-interacting amino groups upon PL adsorption. Carbon-13 spin dynamics studies of side-chain and backbone carbons probe differences between low-frequency motions of bulk-solid and adsorbed polypeptides.

## Experimental Section

**Sample Preparation.** Poly-L-lysine and poly-L-glutamic acid salts were purchased from Sigma Chemical Co. and used as received. PL of viscosity-average molecular weights 3800, 10 200, 25 000, and 69 000 (reported by Sigma), and PG of viscosity-average molecular weights 10 600 and 72 500 (reported by Sigma) were studied. The polypeptides are referred to as PL3.8k, PL10.2k, PL25k, PL69k, PG10.6k, and PG72.5k, respectively. Polydispersities of these polypeptides range from 1.1 to 1.3, as determined by SEC-LALLS and reported by Sigma. Precipitated silica with a reported particle size distribution of 63–200 μm, an average pore diameter of 60 Å, and a BET-measured surface area of 340 $m^2/g$ was obtained from J. T. Baker Inc. (Phillipsburg, NJ). Hydroxyapatite with a reported size distribution of 30–90 μm and a BET-measured surface area of 50 $m^2/g$ was purchased from Bio-Rad Laboratories (HTP grade; Richmond, CA). This material is polycrystalline, with no porosity.[25]

Adsorbed samples were prepared by mixing pH-adjusted aqueous solutions of the polypeptides (prepared in triply distilled, deionized $H_2O$) with pH-adjusted aqueous suspensions of the solid powders. The mixtures were equilibrated with periodic agitation at 0–5 °C for between 60 and 72 h. The pH values of the polypeptide solutions and solid suspensions were adjusted by addition of NaOH or HCl in order to promote adsorption by bringing the surface and polypeptide into oppositely charged states. PL was typically brought to a pH of 7.5 (approximate isoelectric point of amino side chain, 10;[26] of silica, 2;[15] and of hydroxyapatite, 6–7[27]) and PG to a pH of 5.5 (approximate isoelectric point of carboxyl side chain is 4.5[26]). Initial polypeptide concentrations of 10–15 mg/mL generally yielded plateau levels of adsorption on 1 g of solid.

After equilibration, the samples were centrifuged to remove the supernatant and excess polymer, then washed four times by resuspension in pure solvent followed by centrifugation. These wash steps ensured that only chemisorbed polypeptide remained on the surface.[28] Following the final wash, samples were dried at room temperature under flowing nitrogen, then stored at 0–5 °C. Adsorption isotherms were measured subsequently by both thermogravimetric analysis of the solids and UV spectrophotometry of the solutions. Figure 1 shows typical isotherms obtained in this fashion. Although we did not measure complete isotherms for all the different molecular weight polypeptide samples, other investigators show that for these polypeptides under similar adsorption conditions the isotherms are independent of polypeptide molecular weight.[19-20,23] The adsorption amounts we measured for various samples of different molecular weights are consistent with this expectation.

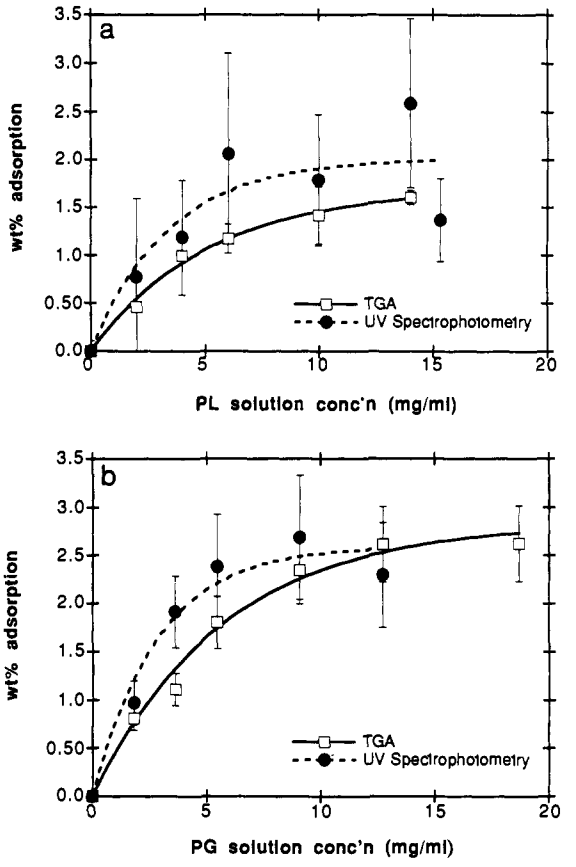


**Figure 1.** Adsorption isotherms of (a) PL3.8k on silica, (b) PG10.6k on HA measured by both thermogravimetric analysis of solids and UV spectrophotometry of supernatants and wash solutions.

In addition to the PL samples adsorbed from solutions at pH 7.5, PL25k and PL69k were also adsorbed onto HA from solutions at pH 11. These samples allow comparison of polypeptides adsorbed from a helical conformation in solution (pH 11) with those adsorbed from a random coil conformation (pH 7.5). The pH dependency of PL solution-state conformation was confirmed with circular dichroism measurements.

A sample of PL3.8k was deuterated at the functional amino groups and adsorbed onto deuterated silica. PL was deuterated at the amino sites through rapid exchange in $D_2O$ while silica was deuterated by first calcining in flowing oxygen at 500 °C for 18 h (to condense SiOH groups and remove surface $H_2O$), then rehydrating in $D_2O$ for 42 h. Excess $D_2O$ was removed by centrifugation and vacuum heating at 100 °C. All pH adjustments were made using NaOD. Equilibration, centrifugation, and washes were performed as described above, using $D_2O$ in place of $H_2O$ in all steps. Handling was done in a glovebag under dry flowing nitrogen to minimize the uptake of atmospheric water.

**Magnetic Resonance.** Carbon-13 cross-polarization magic-angle-spinning (CPMAS) experiments were performed with a Nalorac (Martinez, CA) Quest 4400 solid-state spectrometer and a Doty Scientific (Columbia, SC) double-resonance magic-angle-spinning probe. The operating frequencies were 100.3378 MHz for carbon nuclei and 399.03 MHz for protons. The $^1H$ 90° pulse time was 5.5 μs, with an rf field strength of 45 kHz. Single contact $^{13}C$ CPMAS experiments were performed with quadrature phase cycling and a spin–echo ($\tau$ = 250 μs) refocusing pulse synchronized with the rotor cycles. The spin–echo was

(19) van der Schee, H. A.; Lyklema, J. In *The Effect of Polymers on Dispersion Properties*; Tadros, T. F., Ed.; Academic Press: London, 1982; p 81.

(20) Bonekamp, B. C.; Lyklema, J. *J. Colloid Interface Sci.* **1986**, *113*, 67.

(21) Furusawa, K.; Sakai, H.; Watanabe, N.; Tomotsu, N. *Bull. Chem. Soc. Jpn.* **1983**, *56*, 997.

(22) Furusawa, K.; Kanesaka, M.; Yamashita, S. *J. Colloid Interface Sci.* **1984**, *99*, 341.

(23) Davies, R. J.; Dix, L. R.; Toprakcioglu, C. *J. Colloid Interface Sci.* **1989**, *129*, 145.

(24) Garcia-Ramos, J. V.; Carmona, P.; Hidalgo, A. *J. Colloid Interface Sci.* **1981**, *83*, 479.

(25) Hydroxyapatite particles are nonporous and irregularly shaped while silica particles are porous. It is expected that most of the BET-measured surface area of hydroxyapatite is accessible to the polypeptides. However, because the polypeptide chains in this study range in size from approximately one pore opening (6 nm) to 20 pore openings, much of the silica surface is inaccessible to the polypeptides. (The maximum length of the highest molecular weight polypeptides is approximately 140 nm, and the minimum length of the lowest molecular weight chains is approximately 6 nm.) Thus, the majority of the polypeptide chains see the pores as simply inaccessible holes on the silica surface.

(26) Ciferri, A.; Puett, D.; Rajagh, L.; Hermans, J., Jr. *Biopolymers* **1968**, *6*, 1019.

(27) Chander, S.; Fuerstenau, D. W. In *Solubility and Interfacial Properties of Hydroxyapatite: A Review*; Misra, D. M., Ed.; Plenum Press: New York, 1982; p 29.

(28) Because it is not possible for PG and silica to be oppositely charged at any pH, PG did not adsorb strongly enough on silica to survive the four wash steps.

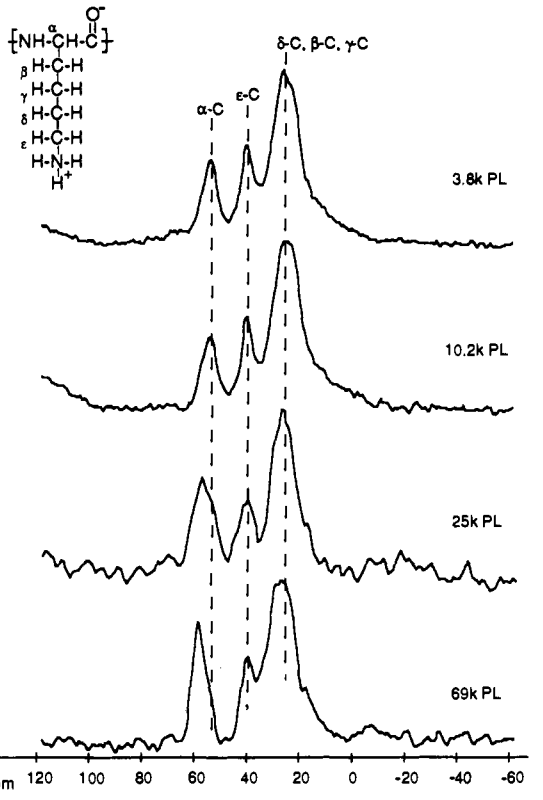


Figure 2. Cross-polarization magic-angle spinning $^{13}C$ spectra of bulk solid PL3.8k, PL10.2k, PL25k, and PL69k. The monomer unit of poly-L-lysine is shown, along with peak assignments.

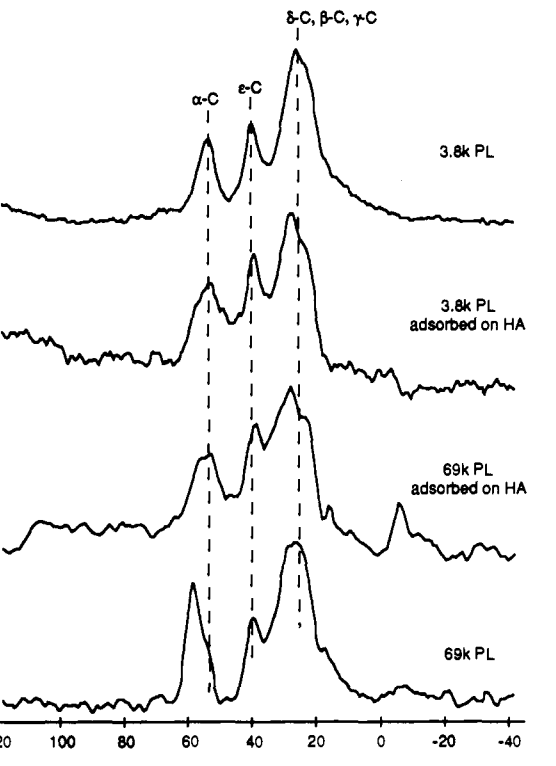


Figure 3. Cross-polarization magic-angle spinning $^{13}C$ spectra of bulk solid and hydroxyapatite-adsorbed PL3.8k and PL69k.

used in order to reduce a large static $^{13}C$ background signal originating from the stator or housing of the probe. Samples were spun in 7-mm (o.d.) sapphire rotors with kel-f end caps. Spinning frequencies were typically 4 kHz, driven by dry nitrogen gas. The volume of the rotors was approximately 0.4 $cm^3$, and 100–150 mg of silica or hydroxyapatite, or 60–100 mg of bulk solid PL or PG, was packed into the rotors.

For typical PL acquisitions, a cross-polarization contact time of 275 $\mu$s and a repetition delay of 0.75 s were used. The contact time was chosen to give maximum methylene carbon excitation before significant proton $T_{1\rho}$ decay. Likewise, a repetition time close to the proton $T_1$ was used to maximize the $^{13}C$ signal for any duration of time-averaging. PG spectra were typically collected with a contact time of 2 ms and a delay of 1.25 s in order to maximize the carboxyl and carbonyl resonances. Good signal-to-noise spectra of bulk polypeptides were obtained in 1000 signal averages. Adsorbed samples, however, required a minimum of 40 000 acquisitions for reasonable spectra. Cross-polarization dynamics were measured by varying the contact time from 10 $\mu$s up to 6 or 7 ms. Carbon-13 $T_{1\rho}$ relaxation was monitored by varying the carbon rotating-frame spin-lock pulse from 0 to 6 or 7 ms. Experiments were normally performed at least twice to ensure reproducibility of the spectra and measured relaxation parameters.

In addition to experiments performed with bulk-solid and adsorbed polypeptides, control experiments were also done on surface particles with no adsorbed polypeptide and on small amounts of solid polypeptide physically mixed with the surface particles. The latter control ensures that the observations of adsorbed polymers are a result of adsorption rather than merely the physical presence of the silica or hydroxyapatite.

Wide-line, low-temperature deuterium spectra were obtained using the same spectrometer described above, operating at 61.2487 MHz, and a home-built variable-temperature, single-resonance deuterium probe. Liquid nitrogen was used for cooling with temperature control to within 2 °C by a Lake Shore Cryotronics (Model DRC 91C) temperature controller. A solid-echo pulse sequence with phase cycling was employed, using a 90° pulse length of 5.3 $\mu$s. The delay between averages was 250 ms. For the wider line spectra, the excitation pulse length was dropped to 4.3 $\mu$s in order to irradiate a wider frequency envelope. Excellent signal-to-noise spectra of bulk PL were obtained within 2400 averages. *Adsorbed PL required more than 500 000 averages for acceptable spectra.*

Carbon-13 and deuterium line shapes were fit quantitatively to various theoretical functions with a nonlinear Newton–Raphson least-squares fitting algorithm. Carbon-13 CPMAS results were fit to Lorentzian functions, whereas deuterium line shapes were fit to superpositions of a Gaussian, Lorentzian, and Gaussian-broadened quadrupolar doublet. Fits to deuterium spectra accounted for finite pulse lengths with a line-shape correction.[29]

## Results

**Carbon-13 Chemical Shifts.** Carbon-13 CPMAS spectra of the four different molecular weight PL samples are presented in Figure 2 with peak assignments taken from the literature.[30] The $\alpha$ peak clearly moves downfield with increasing chain length; a total shift of 4 ppm is observed between the two lower molecular weight polymers and PL69k. The $\alpha$ resonance of PL3.8k appears at 53.7 ppm relative to an external TMS standard; that of PL69k is at 57.8 ppm. The side-chain $\epsilon$ methylene carbon appears at approximately 40.2 ppm in all cases. The broad peak centered near 28 ppm is composed of overlapping resonances from side-chain $\beta$, $\gamma$, and $\delta$ methylene peaks. Shifts of the individual resonances contributing to this peak are not resolved. The PL backbone carbonyl peak (not shown) was not fully excited under the conditions at which these spectra were recorded, so the resonance positions of this carbon were not established accurately.

Figure 3 shows spectra of surface-adsorbed PL3.8k and PL69k, along with the corresponding bulk polymer spectra. The sloping baselines under the PL spectra and the poorly phased peak at −6.5 ppm are background signals partially suppressed with the spin-echo. Shifts in the spectra of the low and high molecular weight adsorbed PL are quite similar, despite the differences seen in the bulk PL spectra of Figure 2. The $\alpha$ resonances of adsorbed PL of both molecular weights appear upfield of that seen in the 69k bulk polypeptide spectrum. The unresolved methylene peaks exhibit greater structural detail, and there is a possible downfield shifting of the $\beta$ resonance away from the $\gamma$ resonance. Also, the $\epsilon$ peak of the adsorbed samples is shifted slightly upfield from that in the bulk PL.

The peak positions (derived from curve fitting) of the $\alpha$ and $\epsilon$ resonances in different molecular weight bulk- and adsorbed-PL are plotted in Figure 4, a and b. The shift in the $\alpha$ peak of low molecular weight adsorbed PL is not significantly different from that in the bulk solid. The same peaks in adsorbed PL25k and

(29) Bloom, M.; Davis, J. H.; Valic, M. I. *Can. J. Phys.* **1980**, *58*, 1510.
(30) Kricheldorf, H. R.; Muller, D. *Macromolecules* **1983**, *16*, 616.

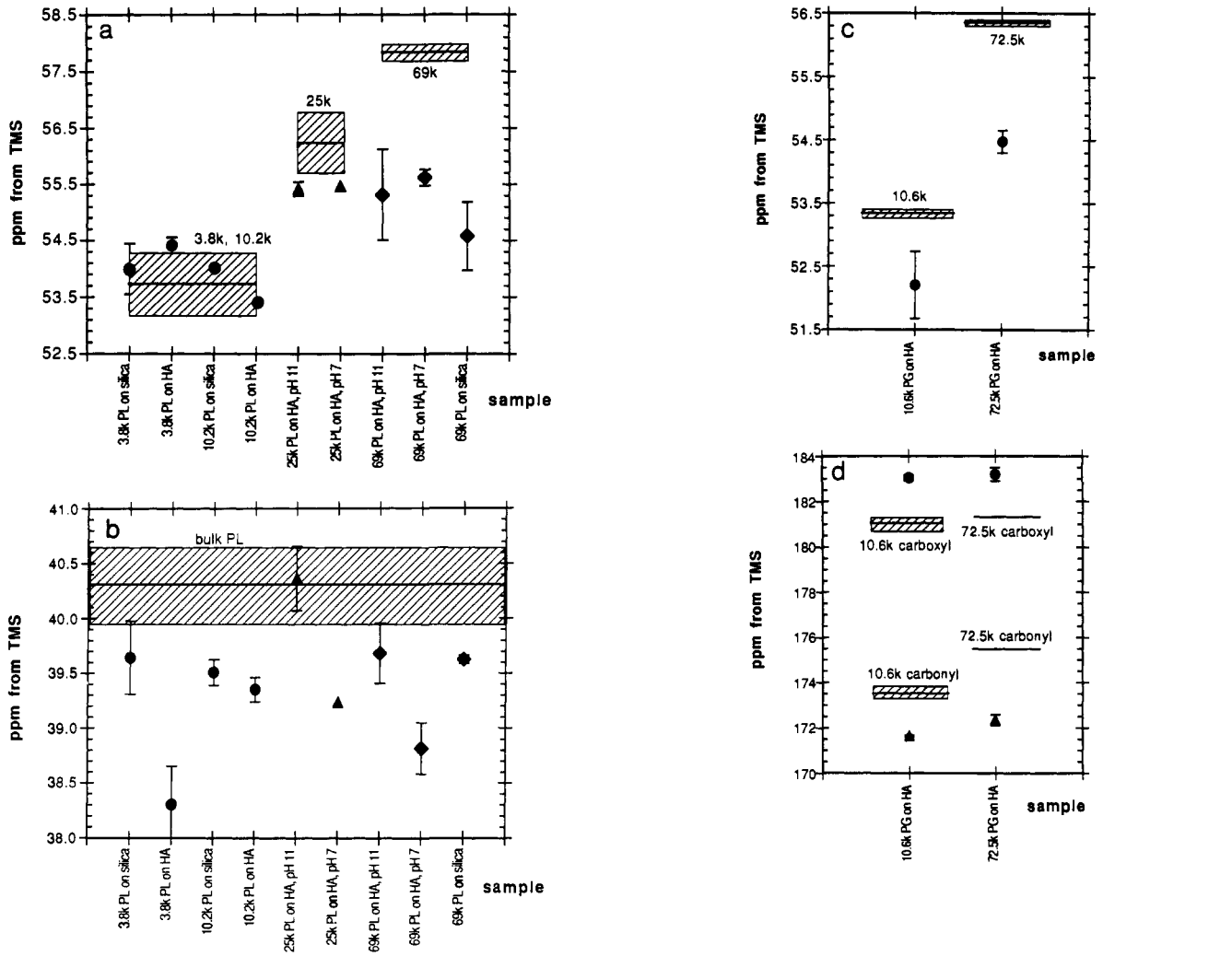


**Figure 4.** Peak positions of $^{13}C$ CPMAS spectra derived from Lorentzian curve fits. Cross-hatched regions show the mean and standard deviations of values obtained for bulk polypeptides. Filled symbols represent shifts of adsorbed polypeptides of various molecular weights, as labeled. Error bars are determined from multiple runs and the uncertainty of the curve fits. (a) $\alpha$ backbone carbon of PL. (b) $\epsilon$ side-chain carbon of PL. The value given for bulk PL is an average of all molecular weight PL samples. (c) $\alpha$ backbone carbon of PG. (d) Carboxyl side-chain and carbonyl backbone carbons of PG.

PL69k, however, are shifted by approximately −0.8 and −2.5 ppm, respectively, in comparison with the bulk state. The $\epsilon$ peak exhibits upfield (more shielded) shifts of approximately −1 ppm in the adsorbed samples.

Spectra of PG10.6k and PG72.5k, in both the adsorbed and bulk solid state, are shown in Figure 5. Comparison of the bulk PG spectra reveals a downfield shift of the backbone $\alpha$ carbon and carbonyl peaks of 3 ppm and 2 ppm, respectively, between the low and high molecular weight PG samples. The side-chain carboxyl peak position does not change with molecular weight. As observed in adsorbed PL, the shifts of PG10.6k and PG72.5k are more similar in the adsorbed state than the bulk solid state. The $\alpha$ and carbonyl resonances of the adsorbed PG are upfield of the corresponding resonances in the bulk solid; the carboxyl peak is shifted downfield in the adsorbed polypeptides.

Figure 4, c and d, shows the curve-fitted peak positions of the $\alpha$ methine, carbonyl, and carboxyl carbons of PG. Upon adsorption the $\alpha$ peak of 10.6k PG shifts −1.1 ppm to 52.2 ppm, and that of 72.5k PG shifts −1.8 ppm to 54.5 ppm. The carbonyl peaks of the low and high molecular weight PG shift −1.9 ppm to 171.6 ppm and −3.2 ppm to 172.3 ppm, respectively. The side-chain carboxyl peak also shifts upon PG adsorption, but in the opposite direction from the $\alpha$ and carbonyl peaks; in both molecular weight adsorbed PG samples, the carboxyl resonance is shifted 2 ppm from approximately 181 ppm to 183 ppm.

**Low-Temperature Deuterium NMR.** A $^2H$ spectrum taken at 200 K of bulk solid PL, deuterated at the side-chain amino group,

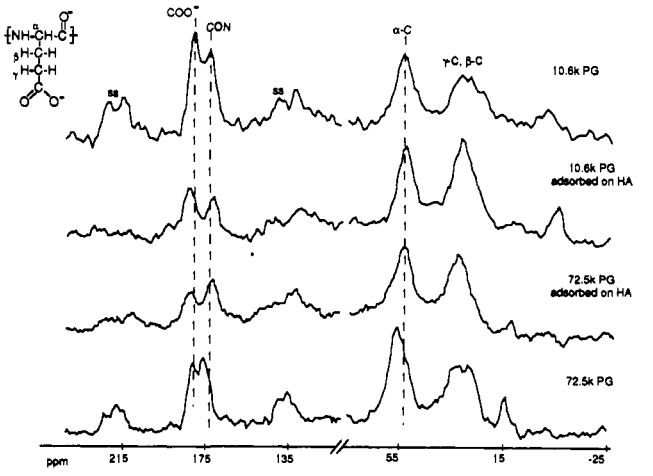


**Figure 5.** Cross-polarization magic-angle spinning $^{13}C$ spectra of bulk-solid and hydroxyapatite-adsorbed PG10.6k and PG72.5k.

is shown in Figure 6a. The fit of the data gives a characteristic quadrupolar doublet splitting of 40.16 kHz. The splitting of a spectrum obtained at room temperature is approximately 35 kHz; at 100 K a 43.7-kHz splitting is observed. The absence of a broad doublet (>100 kHz) in these spectra indicates that no N–D groups are present on the PL backbone.

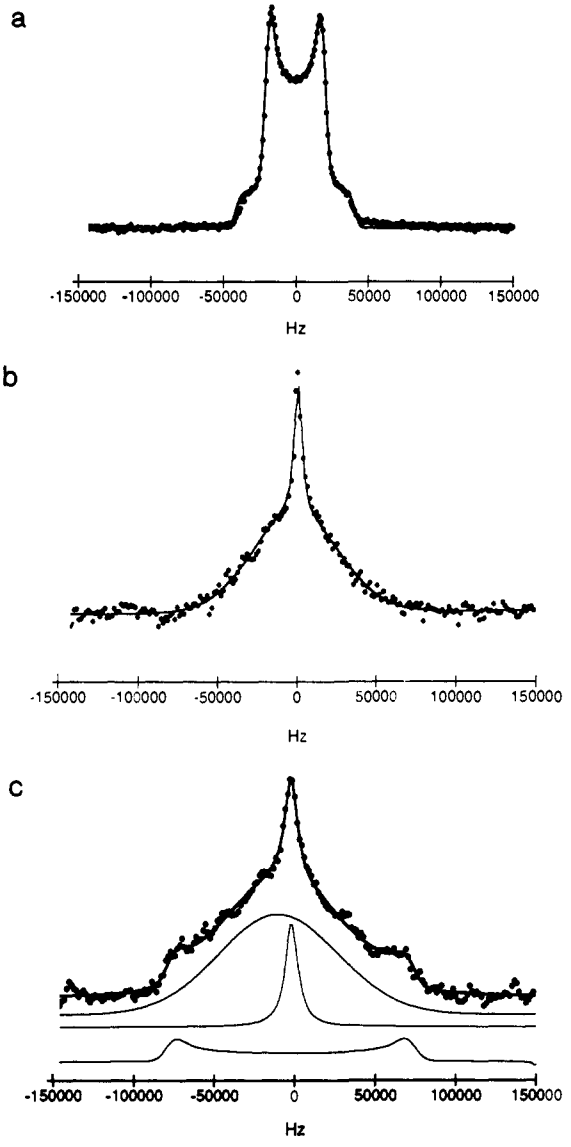


Figure 6. Wide-line deuterium spectra. Data points are shown with dots; numerical fits as described in the text are shown with solid lines. (a) Bulk-solid PL3.8k, deuterated at the side-chain amino groups, at 200 K. (b) Deuterated silica at 250 K. (c) Deuterated PL3.8k adsorbed on deuterated silica, 200 K. Beneath the data are shown, from top to bottom, the Gaussian, Lorentzian, and Quadrupolar powder line shapes which are superimposed to give the fit.

A $^2H$ spectrum of the silica surface at 200 K is predominantly a Gaussian peak with a width of 74 kHz, due to frozen, strongly bound water.[31] At slightly higher temperatures a Lorentzian peak, superimposed on the Gaussian, is evident due to increased mobility of some surface water (Figure 6b). No significant contribution is made from static surface SiOD groups, which would probably appear as a quadrupolar doublet with a splitting of 180–210 kHz,[31] because the groups are largely dissociated at the sample pH and the excitation pulse envelope is not wide enough to fully irradiate the broad line shape.

A spectrum of PL adsorbed on silica, collected with the sample at 200 K, is given in Figure 6c, along with a fit consisting of the superposition of quadrupolar doublet, Gaussian, and Lorentzian line shapes,[32] corrected for the shape of the excitation envelope.[29]

(31) Majors, P. D.; Raidy, T. E.; Ellis, P. D. *J. Am. Chem. Soc.* **1986**, *108*, 8123.

(32) At temperatures higher than 200 K, the adsorbed PL spectrum is dominated by the Lorentzian of mobile surface $D_2O$. Although this mobile component is frozen out at 200 K in silica with no adsorbed PL, a remnant is still present in the sample with adsorbate. This is not surprising considering that silica surface sites on which water would normally adsorb are now occupied by polypeptide amino groups.

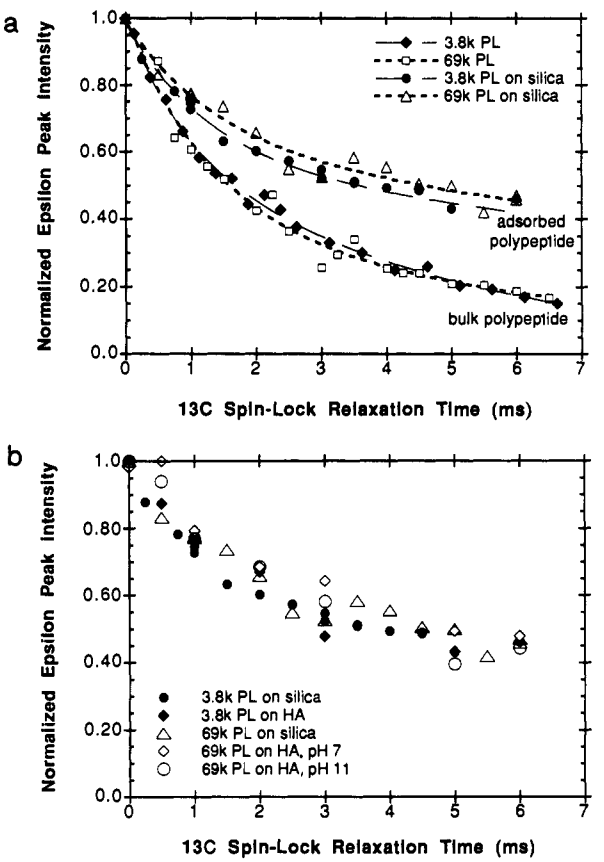


Figure 7. Carbon-13 rotating-frame spin-lock relaxation of the $\epsilon$ side-chain carbon. (a) Bulk-solid and silica-adsorbed PL3.8k and PL69k. Biexponential fits to the decays are included, as described in the legend. (b) PL3.8k and PL69k adsorbed on both hydroxyapatite and silica.

Table I. Results of Biexponential Curve Fits to $^{13}C$ Rotating-Frame Spin-Lock Relaxation Data of the Various Molecular Weight Bulk PL Samples

| | $\alpha$-C | | $\epsilon$-C | | unresolved $CH_2$ | |
|---|---|---|---|---|---|---|
| PL MW | long | short | long | short | long | short |
| a. Long and Short $^{13}C$ $T_{1\rho}$ Time Constants[a] | | | | | | |
| 3.8k | 9.57 | 0.35 | 4.47 | 0.80 | 3.90 | 0.70 |
| 10.2k | 13.45 | 0.65 | 5.33 | 0.97 | 4.75 | 0.63 |
| 25k | 13.71 | 0.84 | 6.30 | 1.26 | 4.88 | 0.68 |
| 69k | 15.12 | 1.06 | 7.46 | 1.30 | 4.94 | 1.05 |
| b. Fractional Contributions to Long and Short $^{13}C$ $T_{1\rho}$ Components | | | | | | |
| 3.8k | 0.88 | 0.11 | 0.66 | 0.34 | 0.70 | 0.28 |
| 10.2k | 0.86 | 0.14 | 0.59 | 0.40 | 0.69 | 0.28 |
| 25k | 0.77 | 0.23 | 0.48 | 0.49 | 0.68 | 0.30 |
| 69k | 0.84 | 0.16 | 0.40 | 0.61 | 0.62 | 0.38 |

[a] In milliseconds.

The fitting parameters of the Gaussian and Lorentzian were derived from fits of the adsorbed water spectra. The intensities and line shapes of the three components of the spectrum are consistent with the assignment of the Gaussian and Lorentzian to surface water and the quadrupolar doublet to the side-chain amino group. The doublet splitting of the adsorbed PL at 200 K is 151 kHz, dramatically larger than the splitting of bulk PL, even at temperatures as low as 100 K.

**Carbon-13 Spin Dynamics.** The rotating-frame magnetization decays ($T_{1\rho}$) of the $\epsilon$ carbon of PL3.8k and PL69k in the bulk-solid state and adsorbed on silica are given in Figure 7a. Similar decays were obtained for the $\alpha$ and unresolved methylene peaks (not shown), and for PL on hydroxyapatite as well (Figure 7b). The decays were found to fit well to a biexponential curve, giving long and short time constants and the fraction of polypeptide contributing to each component of the relaxation (as in ref 33). The

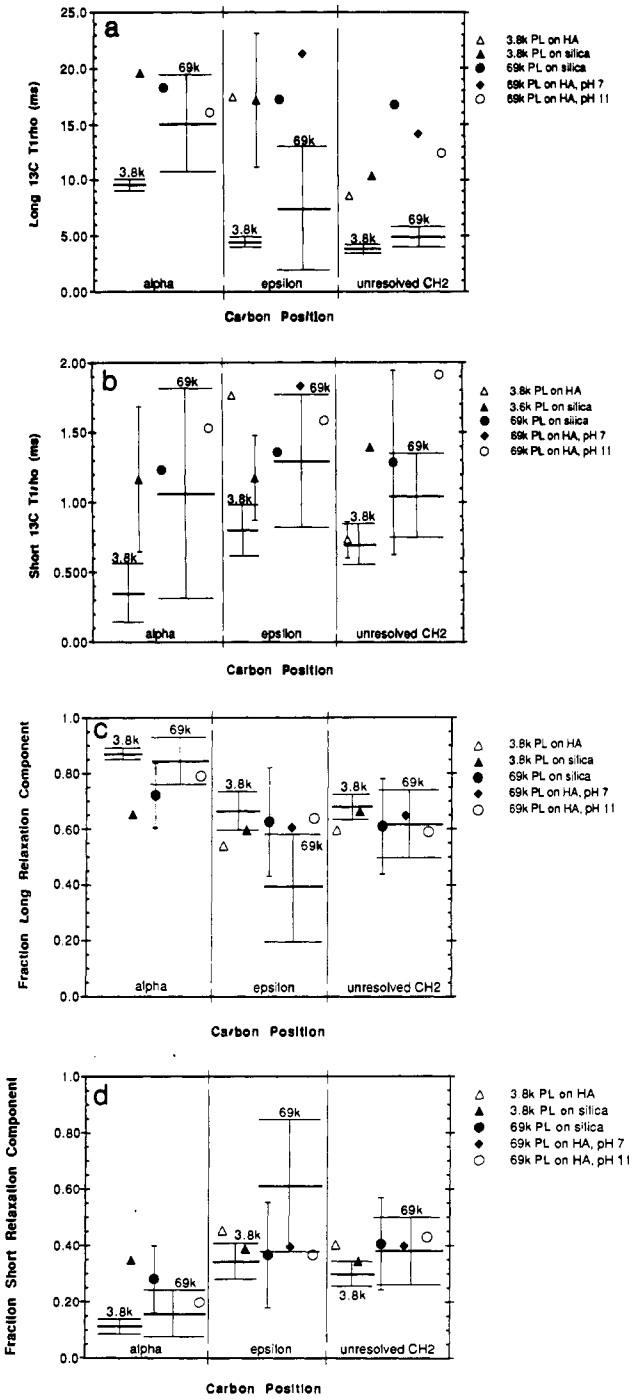


**Figure 8.** (a, b) Long- and short-component $^{13}C$ $T_{1\rho}$ time constants from biexponential curve fits to magnetization decays such as shown in Figure 7. Time constants for $\alpha$, $\epsilon$, and unresolved methylene carbons are shown. The dark horizontal lines represent relaxation times of bulk solid PL3.8k and PL69k, as labeled. Symbols depict relaxation times of adsorbed PL, as described in the legend. Error bars showing the uncertainty of the fits are included for bulk-solid and representative adsorbed PL samples. (c, d) Fractional contributions to the long and short components of $^{13}C$ $T_{1\rho}$ relaxation. Values for bulk solid PL3.8k and PL69k are given with dark horizontal lines, as labeled. Symbols show the fractional contributions for adsorbed samples, as described in the legend. Representative uncertainty estimates are included.

results of the fits for the different molecular weight solid polypeptides are given in Table Ia,b; curve fit results for adsorbed PL samples are depicted graphically in Figure 8. The range of $\chi^2$ values was $10^{-4}$ to $10^{-2}$. The correlation coefficient, $R$, was at least 0.98 for bulk polypeptide measurements and a minimum of 0.93 for measurements of adsorbed polypeptides. Despite good fits, accurate parameters of the fits could not be obtained with great certainty for the samples adsorbed on hydroxyapatite because of the small number of data points collected (7 as opposed to 13 to 20). The decays are, however, essentially the same as those for PL adsorbed on silica, as shown in Figure 7b for the $\epsilon$ carbon. Although the uncertainties in the fitted parameters of the samples adsorbed on HA are high, parameters from fits giving a $\chi^2$ value of at most 0.04 are included in Figure 8.

**Table II.** $T_{1/2}$ Values (in microseconds) of Carboxyl and Carbonyl Carbons in Bulk Solid and Hydroxyapatite-Adsorbed PG10.6k and PG72.5k[a]

| | PG10.6k | | PG72.5k | |
|---|---|---|---|---|
| | bulk | adsorbed on HA | bulk | adsorbed on HA |
| carbonyl | 145 | 60 | 153 | 82 |
| carboxyl | 180 | 150 | 165 | 100 |

[a] Uncertainties in reported values are 10–15%.

In general, there is a greater fraction of long-component $^{13}C$ $T_{1\rho}$ relaxation than short-component; this fraction appears to diminish with increasing PL chain length. The decrease is particularly dramatic in the $\epsilon$ carbon resonance. With the possible exception of the short-component unresolved methylene peak, both short and long $T_{1\rho}$ relaxation time constants clearly increase with increasing PL molecular weight (and thus, decreasing chain mobility). The changes are considerably more substantial in the slower relaxing component, and the $\alpha$ methine carbon is affected most strongly.

The magnetization decays of the adsorbed PL are generally significantly slower (longer relaxation time constants) than of the bulk solids, especially in the side-chain $\epsilon$ carbon. This behavior is most apparent in the long $^{13}C$ $T_{1\rho}$ components, and is also evident in the short-relaxation components. Of the long components, only the relaxation of the $\alpha$ carbon of PL69k is not greatly diminished upon adsorption. Also, except for the adsorbed PL69k $\epsilon$ and perhaps unresolved methylene resonances, the adsorbed samples generally exhibit a smaller fraction of long-to-short relaxation components than do the bulk samples. The trend in the adsorbed PL69k $\epsilon$ carbon is clearly opposite of the general trend. As was seen in the chemical shift data, the rotating-frame relaxation behavior of all samples in the adsorbed state are more similar than as bulk solids.

Comparable data to those presented for PL were also obtained for PG. However, the PG decays were modulated by small oscillations. Additionally, relaxation of the side-chain peaks was considerably slower in PG due to the hindered motion of bulky carboxyl side groups.[34] The carbonyl and carboxyl magnetization do not decay more than 10% in the first 6 or 7 ms of carbon spin lock. These characteristics make it difficult to determine the $^{13}C$ $T_{1\rho}$ relaxation times of PG quantitatively. The time constant for magnetization transfer during cross polarization is also sensitive to polymer motional parameters[9,35] and proved more useful than $^{13}C$ $T_{1\rho}$ for analysis of PG motion.

Figure 9, a and b, shows the rise in magnetization of the carbonyl and carboxyl peaks of bulk and adsorbed PG during spin-lock cross polarization. The bulk PG data exhibit rises in magnetization consistent with a system in which the homonuclear $^1H$–$^1H$ coupling dominates over the $^{13}C$–$^1H$ coupling.[36,37] The polarization transfer rises of the adsorbed PG samples, however, are clearly nonexponential, reflecting an increase in $^{13}C$–$^1H$ coupling relative to $^1H$–$^1H$ coupling.

The time at which the magnetization reaches one-half of its maximum value, $T_{1/2}$, was measured for the various PG reso-

(33) Connor, T. M. In *Magnetic Relaxation in Polymers. The Rotating Frame Method*; Diehl, P., Fluck, E., Kosfeld, R., Eds.; Springer Verlag: New York, 1971; p 247.

(34) Hahn, U.; Hanssum, H.; Ruterjans, H. *Biopolymers* **1985**, *24*, 1147.
(35) Tuel, A.; Hommel, H.; Legrand, A. P.; Balard, H.; Sidqi, M.; Papirer, E. *Colloid Surf.* **1991**, *58*, 17.
(36) Cheung, T. T. P.; Yaris, R. *J. Chem. Phys.* **1980**, *72*, 3604.
(37) Muller, L.; Kumar, A.; Baumann, T.; Ernst, R. R. *Phys. Rev. Lett.* **1974**, *32*, 1402.

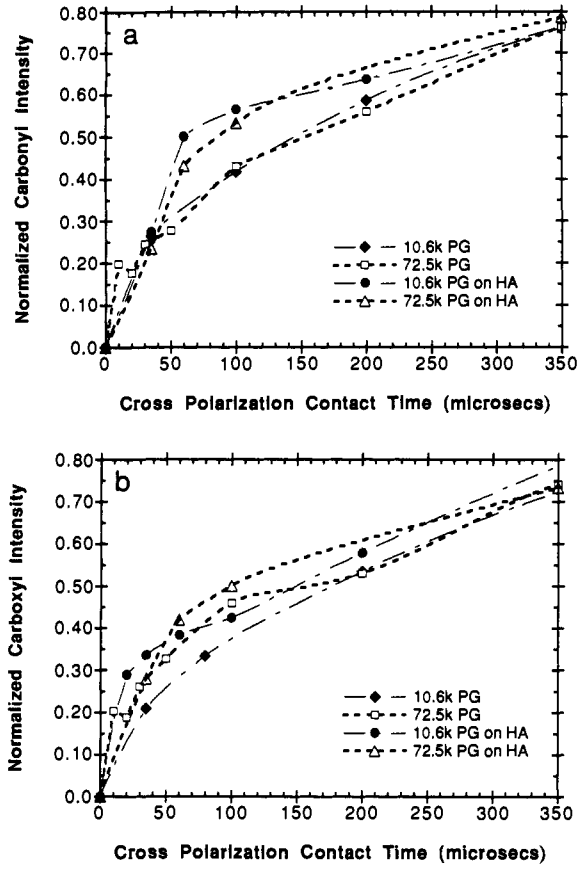


Figure 9. Rise in $^{13}C$ magnetization during spin-lock cross-polarization of bulk solid and adsorbed PG10.6k and PG72.5k, as indicated on the legend. Data points were collected up to 6 or 7 ms, but for clarity only the early rise times are shown: (a) carbonyl carbon, (b) carboxyl carbon.

nances. Because of the fast stepwise rises in intensity of the methylene and methine peaks, $T_{1/2}$ of these carbons could not be accurately determined. It is approximately 10 to 20 $\mu$s in all cases, which falls in the range expected for methylene carbons of polymers.[38] $T_{1/2}$ times could, however, be more accurately measured in the slower rising carboxyl and carbonyl resonances, and are given in Table II. Since $T_{1/2}$ is determined from an interpolated curve rather than a fit to a function, the uncertainties in the reported values are probably 10–15%. Within the limits of certainty, $T_{1/2}$ values of both low and high molecular weight PG are the same. The carboxyl carbon is described by a longer $T_{1/2}$ than the carbonyl. Upon adsorption, the $T_{1/2}$ values of both PG10.6k and PG72.5k decrease; in contrast to adsorbed PL, greater changes are seen in the backbone than the side-chain time constants.

## Discussion

Considerable work has been done in recent years on conformation dependent chemical shifts of polypeptides, including PG and PL.[30,39-42] It is now well established that the $\beta$-sheet to $\alpha$-helix transformation in peptides results in downfield (higher frequency) shifts of the backbone $\alpha$ and carbonyl carbon resonances, and upfield shifts of the $\beta$ carbon peak. Shifts of up to 7 ppm have been observed. Other carbon groups are unaffected by changes in the polypeptide secondary structure. These results have been documented for a large number of both solution- and solid-phase polypeptides.

The chemical shift data for bulk PL are presented in Figures 2 and 4. The solid PL69k $\alpha$ carbon resonance, at 57.8 ppm, compares well with literature values of 57.4 and 57.6 ppm for PL in the $\alpha$-helical conformation.[30,41] The $\alpha$ resonance of the shorter chain length PL samples, at 53.7 ppm, is closer to literature values for the $\beta$-sheet (51.4 ppm and 52.3 ppm[30]) than the $\alpha$-helix. Resonances appearing between the $\alpha$-helix and $\beta$-sheet extremes are known to contain some random coil character.[39] The absence of a chemical shift of the side-chain $\epsilon$ methylene group with changing PL molecular weight is consistent with the observations of many researchers showing that only the $\alpha$, carbonyl, and $\beta$ shifts are affected by polypeptide secondary structure.[41] While the $\beta$ peak has been observed to move upfield by almost 1 ppm with $\alpha$-helix formation,[30,41] these shifts could not be resolved in this study.

The data for bulk solid PG in Figures 4 and 5 can be interpreted similarly. The $\alpha$ peak of PG72.5k, at 56.3 ppm, corresponds to the $\alpha$-helix peak positions of 56.8, 56.4, and 56.74 ppm reported in the literature.[30,42,43] The corresponding peak in the PG10.6k sample at 53.3 ppm is between the resonance positions for the fully extended $\beta$-sheet (51.3 ppm[30]) and the $\alpha$-helix. The carbonyl resonance of PG72.5k at 175.5 ppm also corresponds to literature values for the helical conformation (175.6 ppm and 175.4 ppm),[30,42,43] while the position of the same peak in PG10.6k at 173.5 ppm is consistent with more extended structure (172.6 ppm[30]).

The downfield shifts of the backbone $\alpha$ and carbonyl $^{13}C$ resonances with longer average polypeptide chain length show the increasing degree of helicity of the higher molecular weight polymers. This behavior has been widely demonstrated for polypeptides in both solution and the solid state.[44] The resonances of PL69k and PG72.5k are consistent with literature values for nearly 100% helical structures, while those of the low molecular weight PL3.8k and PG10.6k are not as far upfield as expected for 100% extended $\beta$-sheet structure. Thus, the shorter chain length polypeptides are best characterized as random coil with some extended B-sheet or helical structure, while the longer chains appear to be mostly $\alpha$-helical. With appropriate pH conditions, these solid-state polypeptide structures are qualitatively retained in solution, as was confirmed with circular dichroism experiments. The solutions (from which the polypeptide was adsorbed) of low molecular weight PL are predominantly random coil, as shown by positive $\epsilon$ values at 220 nm; the PG10.6k solution reveals some helical character with a small negative peak near 222 nm. Large negative $\epsilon$'s in the vicinity of 222 nm in the high molecular weight PG72.5k solution confirms a mostly helical conformation. A predominantly helical conformation is present in pH 11 solutions of PL25k and PL69k; these conformations change to random coil at pH 7.5.

The chemical shifts of the $\alpha$ and/or carbonyl peaks of all adsorbed polypeptides, regardless of solution conformation or surface, show a loss of helicity and a trend toward the more extended structure upon adsorption. Only the $\alpha$ peak of the shortest chain PL does not shift significantly upfield from its position in the bulk solid, indicating that the bulk extended conformation of the short chain is retained on the surface. Shifts of PL adsorbed from solutions of *either* $\alpha$-helix or random coil conformation are virtually identical in the adsorbed state. The peak behavior in the region of the unresolved $\gamma$, $\delta$, and $\beta$ methylene peaks of the adsorbed PL spectra is difficult to pinpoint because of the overlapping resonances. However, the greater structural detail in this region compared with the bulk PL spectra may be due to a downfield shift of the $\beta$ methylene group away from the $\gamma$ peak; such behavior is also consistent with the loss of helical secondary structure.

The observed shifts in the $\epsilon$ methylene group of adsorbed PL by an average of about 1 ppm indicate a direct interaction of the

(38) Laupretre, F.; Monnerie, L.; Virlet, J. *Macromolecules* **1984**, *17*, 1397.
(39) Saito, H.; Tabeta, R.; Shoji, A.; Ozaki, T.; Ando, I. *Macromolecules* **1983**, *16*, 1050.
(40) Saito, H.; Tabeta, R.; Shoji, A.; Ozaki, T.; Ando, I.; Miyata, T. *Biopolymers* **1984**, *23*, 2279.
(41) Saito, H. *Magn. Reson. Chem.* **1986**, *24*, 835.
(42) Shoji, A.; Ozaki, T.; Saito, H.; Tabeta, R.; Ando, I. *Macromolecules* **1984**, *17*, 1472.
(43) Pivcova, H.; Saudek, V.; Schmidt, P.; Hlavata, D.; Plestil, J.; Laupretre, F. *Polymer* **1987**, *28*, 991.
(44) Bamford, C. H.; Elliott, A.; Hanby, W. E. *Synthetic Polypeptides. Preparation, Structure, and Properties*; Academic Press: New York, 1956

adjacent side-chain amino group with the surface. The shift is not related to the conformational change, as shown previously by other researchers.[41] The upfield shift demonstrates greater shielding of the carbon group, which is consistent with its coming into the vicinity of a negatively-charged surface site.[45] The similar behavior of PL adsorbed on both hydroxyapatite and silica supports the hypothesized electrostatic adsorption mechanism since, except for the presence of negatively-charged surface sites ($SiO^-$ or $H_2PO_4^-$), the chemistries of the surfaces are quite different. The 2-ppm downfield shift of the carboxyl group of adsorbed PG also indicates direct interaction of the side-chain functional group with the surface. The slightly-larger shift than that of the $\epsilon$ carbon of PL is consistent with the direct interaction of this group with the surface. The direction of the shift indicates decreased shielding of the group, which can be explained by its interaction with positively-charged surface sites which pull the electron cloud away from the carboxyl carbon. The identical shifts of the side-chain carboxyl group in both the high- and low-molecular weight PG samples, and the lack of any trend with PL molecular weight in the shifting side-chain $\epsilon$ group, suggest that most of the side chains interact with the surface at identical sites and few loops or tails exist.[46]

The deuterium data appearing in Figure 6 reveal further details regarding side-chain interactions with the surface. Direct interaction of the PL side-chain amino groups with surface sites is verified in the line shapes of deuterium spectra. The small frequency splitting separating the singularities in the deuterium quadrupolar doublet of bulk-solid PL demonstrates the rapid rotational motion about the $C_3$ axis of the functional group. Upon direct interaction of the amino group with negatively-charged surface sites, the rotational rate becomes severely restricted and the quadrupolar splitting more than doubles. This restriction in motion is not achieved in the bulk polypeptide even at temperatures as low as 100 K.

In addition to fast local motions such as the amino group rotation, macromolecular dynamics are also characterized by slow, cooperative backbone chain motions. Solid-state NMR has been used extensively to describe this behavior in bulk polymers through the measurement of relaxation times which are sensitive to lower frequency kilohertz range motions. Carbon-13 CPMAS has been especially useful because the low natural abundance of the $^{13}C$ isotope allows for effective isolation of the nuclei, thus enabling the motional states of individual carbon resonances to be resolved. Motions of side-chain carbons are therefore easily resolved from those of backbone carbons. The $^{13}C$ rotating-frame relaxation, $^{13}C$ $T_{1\rho}$, and the characteristic measure of spin-lock cross-polarization dynamics, $T_{1/2}$, have both been applied in investigations of the motional states of bulk polymers.[38,43,47] While cross-polarization dynamics has been measured in studies of motion in long-chain molecules grafted on silica,[8,9] neither relaxation parameter has been previously measured in surface-adsorbed polymers.

It has been shown that the $^{13}C$ $T_{1\rho}$ relaxation in polymers may contain contributions from both spin–spin and spin–lattice relaxation mechanisms.[48] The spin–lattice relaxation mechanism occurs via interactions with fluctuating magnetic fields generated by local motions of nearby nuclei. The spin–spin relaxation results from interactions with fluctuating fields generated by mutually flipping proton spin pairs. Considerable effort has gone into separating the effects of these two mechanisms in studies of polymer dynamics;[48] this is unnecessary in this study since only relative relaxation rates within a particular polymer are of interest. Changes in the rate of either mechanism are caused by changes in motion, which either directly affect the local nuclear motion or alter the local proton dipolar field. While the spin–spin relaxation mechanism may also be affected by changes in proton spatial distribution resulting from polypeptide conformational changes, this is unlikely to be of significance in carbon nuclei with directly-bonded protons. The presence of a large $^{13}C$ $T_{1\rho}$ change between bulk and adsorbed PL3.8k despite similar conformations (as shown in the chemical shift results) further supports that motional rather than conformational effects are the dominant mechanisms of $^{13}C$ $T_{1\rho}$ relaxation in these systems. Changes in either frequency or amplitude of motion are manifested in the same way in these experiments. Thus, while the experiments can resolve differences in motion, they cannot specify whether the changes are in the frequency or amplitude of the motion. The rate of magnetization transfer in the cross-polarization experiment is also sensitive to molecular motion and (in the case of carbons with nonbonded protons) spatial distribution of protons. The cross-polarization efficiency relies on the strength of the $^1H$–$^{13}C$ dipolar interaction, which is related directly to molecular motion. Greater motion averages the coupling strength and decreases cross-polarization effectiveness, thus lengthening the time constant. In contrast, constrained motion allows for a stronger $^1H$–$^{13}C$ coupling and a faster magnetization transfer.

The $^{13}C$ $T_{1\rho}$ data are presented in Figures 7 and 8 and Table I. The $^{13}C$ $T_{1\rho}$ decay has been characterized as multiexponential in many polymer systems owing to multiple phases present in the solid.[47] For PL and PG, the biexponential function indicates two dominant relaxation mechanisms. *In the bulk-solid polypeptides* the relaxation efficiencies of both mechanisms are lower in samples of greater molecular weight. This demonstrates that, with the decreasing mobility associated with increasing polypeptide chain lengths, relaxation by the $^{13}C$ $T_{1\rho}$ mechanisms loses efficiency, and both components of $T_{1\rho}$ lengthen. Thus, the relaxation is characterized by the slow-motion side of the $T_{1\rho}$ minimum. The greater effect on the backbone $\alpha$ carbon relative to the side-chain carbons is expected since mobility of the main chain is the most sensitive to chain length. We speculate that because the relative fraction of fast relaxing component generally increases with increasing chain length, it is most likely associated with the growing ordered phase of the polymer. The slower relaxing component probably reflects the more mobile, amorphous regions of the chain.

The relaxation time data of the adsorbed PL show several interesting trends. The slower component $^{13}C$ $T_{1\rho}$ relaxation times of the adsorbed PL side-chain carbons are up to three times longer than those of the bulk solids. As shown by the trends seen in the bulk PL samples, this reduced relaxation efficiency is caused by a dramatic restriction in PL side-chain mobility upon adsorption. The slow component of the main chain $\alpha$ carbon in PL3.8k increases with adsorption, but that of the PL69k is only slightly changed. This indicates that the backbone mobility of PL3.8k is decreased when adsorbed, whereas that of PL69k remains essentially unchanged. The similar $^{13}C$ $T_{1\rho}$ relaxation parameters of adsorbed PL3.8k and PL69k show that the two molecular weight polypeptides share similar motional behavior when adsorbed on silica or HA, despite their widely differing behavior as bulk solids.

Together with the conformational changes deduced from the polypeptide chemical shifts, the rotating-frame relaxation time results allow us to conclude that PL chains adsorb on silica and HA in an extended conformation via strong electrostatic interactions of side-chain amino groups with the surfaces. Side-chain mobilities are restricted substantially by adsorption; the main chain mobilities, however, appear to be changed only in the lower molecular weight (shorter chain length) PL. Thus the backbone mobility of adsorbed molecules is probably less than that of bulk solid PL3.8k in the $\beta$-sheet/random coil configuration, yet about as rigid as the $\alpha$-helical conformation seen in bulk PL69k.

Because the measured $T_{1/2}$ of carboxyl and carbonyl peaks may be affected by either or both molecular motion or spatial distribution of nonbonded protons, the interpretation of the data is somewhat ambiguous. In view of the other motional results thus far presented, however, the $T_{1/2}$ results on carboxyl and carbonyl peaks of PG and adsorbed PG may be used to support a similar

(45) Chiang, C.-H.; Liu, N.-I.; Koenig, J. L. *J. Colloid Interface Sci.* **1982**, *86*, 26.

(46) Fleer, G. J.; Lyklema, J. In *Adsorption of Polymers*; Parfitt, G. D., Rochester, C. H., Eds.; Academic Press: London, 1983; p 153.

(47) Schaefer, J.; Stejskal, E. O.; Buchdahl, R. *Macromolecules* **1977**, *10*, 384.

(48) Schaefer, J.; Sefcik, M. D.; Stejskal, E. O.; McKay, R. A. *Macromolecules* **1984**, *17*, 1118.

picture of the polypeptide adsorption. If $T_{1/2}$ is more indicative of motion than proton distribution, decreased $T_{1/2}$ upon PG adsorption demonstrates a loss in motional freedom of both the polypeptide side chain and backbone, with the effect being largest on main chain carbonyl motion. Adsorbed PG is thus also proposed to be a nonhelical structure, rigidly attached to the surface via side-chain carboxyl functional groups.

## Conclusions

Structural and dynamic information for poly-L-lysine and poly-L-glutamic acid adsorbed on hydroxyapatite and/or silica has been obtained successfully with standard solid-state NMR experiments. Chemical shifts of main chain $\alpha$ and carbonyl resonances show that the helical character of the polypeptides is greatly reduced upon adsorption. Shifts of side-chain $\epsilon$ and carboxyl carbon peaks demonstrate that the mechanism of adsorption is via side-chain functional group interactions with the surfaces. Deuterium experiments quantify the extent of motional restriction of the rotating amino group upon PL adsorption. Relaxation of the carbon magnetization, characterized in PG with $T_{1/2}$ and in PL with $T_{1\rho}$, shows a dramatic reduction in motional freedom of the side chains when the polypeptide is adsorbed. Motional freedom of the adsorbed backbone seems to be reduced in both PG and the lower molecular weight PL samples, but unchanged in the high molecular weight PL.

The conformation and mobility of PL and PG adsorbed on the studied surfaces are at least qualitatively independent of polypeptide molecular weight and bulk-solid and solution conformations. This is in contrast to the differences in conformation and mobility observed in bulk-solid polypeptides or different molecular weights. From the results of this investigation, it is proposed that the polypeptides adsorb in relatively extended, nonhelical chains, strongly bound to the surface via electrostatic interactions between the side-chain functional groups and charged surface sites.

**Acknowledgment.** This work was supported in part by the Director, Office of Energy Research, Office of Basic Energy Sciences, Materials Sciences Division of the U.S. Department of Energy under Contract No. DE-AC03-76SF00098. V.L.F. also acknowledges the generous fellowship support of the National Science Foundation and fellowship and research-expense awards from the Graduate Division, University of California at San Francisco. The authors express gratitude to Lynne Kawakami for assistance with sample preparation and characterization.

**Registry No.** Poly-L-lysine homopolymer, 25104-18-1; poly-L-lysine SRU, 38000-06-5; poly-L-glutamic acid homopolymer, 25513-46-6; poly-L-glutamic acid SRU, 24991-23-9; silica, 7631-86-9; hydroxyl apatite, 1306-06-5.